

FMR evidence of strong uniaxial anisotropy in $\text{La}_{1-x}\text{Ca}_x\text{MnO}_3$

C.A. Ramos, E. Winkler, and M.T. Causa
Centro Atómico Bariloche e Instituto Balseiro,
Bustillo 9500, S.C. de Bariloche, 8400 Río Negro, Argentina.
e-mail: c Ramos@cab.cnea.gov.ar

Recibido el 25 de junio de 2010; aceptado el 20 de octubre de 2010

We report an electron spin resonance study on $\text{La}_{1-x}\text{Ca}_x\text{MnO}_3$ ceramic samples with $x = 0.33$ and 0.5 . Below T_C the absorption line-shape can be well described as a ferromagnetic resonance with randomly distributed uniaxial anisotropy. In both samples the line-shape is used to fit an average anisotropy value. The anisotropy changes from easy plane for $x = 0.33$ to easy axis for $x = 0.5$. The present results for $x = 0.5$ imply that the uniaxial anisotropy, obtained from the measurements at 100K , is larger than the one expected for shape-only contribution even considering the extreme case of nanowires. The origin and magnitude of this anisotropy are discussed.

Keywords: Ferromagnetic resonance; electron spin resonance; $\text{La}_{1-x}\text{Ca}_x\text{MnO}_3$; manganites; uniaxial anisotropy.

Presentamos un estudio mediante resonancia electrónica de espín en muestras cerámicas de $\text{La}_{1-x}\text{Ca}_x\text{MnO}_3$ con $x = 0.33$ y 0.5 . Por debajo de T_c la línea de absorción puede describirse como una resonancia ferromagnética con eje de anisotropía uniaxial distribuido al azar. En ambas muestras la forma de línea se usa para ajustar una anisotropía promedio. La anisotropía cambia de plano fácil, para $x = 0.33$ a eje fácil para $x = 0.5$. Los resultados para $x = 0.5$ implican que la anisotropía uniaxial, obtenida de mediciones a 100K , es mayor que la esperable para contribuciones debidas sólo a la forma, aún considerando el caso extremo de nanohilos. El origen y la magnitud de esta anisotropía son discutidas.

Descriptores: Resonancia ferromagnética; resonancia de electron de espin; $\text{La}_{1-x}\text{Ca}_x\text{MnO}_3$; manganitas; anisotropía uniaxial.

PACS: 76.50.+g, 71.30.+h, 75.47.Lx, 75.30.Gw

1. Introduction

For over a decade a large effort has been devoted to understanding the physics of colossal magnetoresistant materials, particularly manganites, where electron-doping, structure and magnetic order are intimately linked to determine its properties [1, 2]. The phase diagram as a function of doping and temperature can present metallic-insulating transitions often associated to ferromagnetic-paramagnetic (FM-PM) or FM-antiferromagnetic (AFM) states, charge-ordered regions, and intrinsic phase coexistence (PC) where lattice effects play a significant role [1-6].

One of the most intensively studied manganites is the $(\text{La,Ca})\text{MnO}_3$. Indeed $\text{La}_{1-x}\text{Ca}_x\text{MnO}_3$ phase diagram presents a ferromagnetic-metallic phase for $0.23 < x < 0.5$ below the transition temperature (between $\sim 200\text{K}$ for $x = 0.23$ and $\sim 270\text{K}$ for the optimally-doped $x = 0.33$) and an antiferromagnetic charge-ordered insulating phase for $0.5 < x < 0.9$. For a narrow region around $x = 0.5$ the FM-AFM phases have been found coexist [2, 7].

Several techniques have been used to establish this FM-AFM coexistence. The first evidence was derived from neutron scattering [8] applied to $\text{La}_{1-x}\text{Ca}_x\text{MnO}_3$ with $x = 0.18$, which indicated the coexistence of FM and AFM phases. Nuclear magnetic resonance (NMR) yields local information on the magnetic ordering surrounding the nucleus under study. The AFM or FM arrangement can be distinguished by its frequency dependence with the applied field [9]. The NMR results indicate the presence of both, AFM and FM phases below 4K for $x = 0.5$. As a local probe this technique is not sensitive to the extent of the AFM-FM domains.

TEM results [7,10] in $\text{La}_{0.5}\text{Ca}_{0.5}\text{MnO}_3$ indicate the presence of inhomogeneous spatial mixture of charge ordered and FM domains of sub-micrometric size coexisting. Mesoscopic phase coexistence of insulating charge-ordered and conducting charge-disordered in a $\text{Bi}_{0.24}\text{Ca}_{0.76}\text{MnO}_3$ crystal has been determined by STM and atomic resolution I(V) curves [11]. Based on experimental and theoretical results a phase diagram for $\text{La}_{1-x}\text{Ca}_x\text{MnO}_3$ that includes coexistence regions [12] has been proposed.

The magnetic properties of manganites are routinely measured using magnetization measurements. However, in this experiment it is difficult to quantify paramagnetic (PM) portion from the total magnetic moment in a FM-PM phase coexistence. This quantification can be carried out using electron spin resonance (ESR), where the FM and PM contributions can be separately quantified [13-21]. Additionally, the ESR linewidth can be directly related to the crystal environment and the magnetic susceptibility [22] in the paramagnetic regime, and to the magnetic anisotropy in the ferromagnetic state.

In the study of FM-AFM/PM region at the μm level ESR yields relevant information as the typical exchange length in a ferromagnet is $\sim 10\text{ nm}$. In the ordered state ESR can be used to characterize single crystals [23,24], determine the shape and crystalline anisotropy of different origins separately [25,26], and to study magnetic nanoparticles [27,28]. Additionally, the metallic character of the sample modifies the ESR lineshape. Indeed, when the microwave skin depth is smaller than the minimum sample dimension, a dysonian lineshape is observed in the PM state, and gives rise to antiresonance in the FM state [24,29].

In this work we present an ESR study of $\text{La}_{1-x}\text{Ca}_x\text{MnO}_3$ with $x = 0.5$, where FM-AFM phase segregation is expected, and a sample with $x = 0.33$, which is FM and metallic at low temperature. We compare the results and analyze the origin of the anisotropy field present in each case.

2. Experimental

For this study we used ceramic samples of $\text{La}_{1-x}\text{Ca}_x\text{MnO}_3$, $x = 0.33$ and 0.5 , synthesized by solid-state reaction. Room temperature x-ray diffraction patterns indicate that the samples are single phase (orthorhombic, *Pnma*) [30,31]. Successive annealing at 1300°C during 60, 50 and 100 h were performed, grinding and pressed after each cycle. The sample grain size was typically larger than $5\ \mu\text{m}$. The samples used in the ESR experiments were ground from bulk ceramics into a fine powder. The ESR experiments were performed in a ESR 300 Bruker spectrometer operating at Q band (34.3 GHz) and X band (9.4 GHz). The experiments were performed between 100 and 340 K. In the Q-band experiment the temperature was monitored with a Fe/Au thermocouple introduced into the 1 mm diameter tube used as a sample holder at about 2.5 cm away from the sample. This assured the temperature reading was within a fraction of a degree from the sample temperature. For calibration purposes we included a DPPH g-marker. All the ESR measurements reported here were taken after cooling down to the lowest temperature at zero field. The convenience of using the Q-band for performing the ESR experiments is determined from the fact that a moderately large uniaxial anisotropy, such as the one observed in this work, modify drastically the lineshape and intensity of the spectra [17,30].

3. Results and discussion

Before presenting the ESR measurements, we are going to introduce the resonance condition derived from the Smith-Beljers equation [32]. For a ferromagnetic case with uniaxial anisotropy the ferromagnetic resonance (FMR) condition is obtained:

$$\left(\frac{\omega}{\gamma}\right)^2 = \frac{[H_R \cos \phi + H_A \cos^2(\phi - \phi_n)]}{[H_R \cos \phi + H_A \cos(2(\phi - \phi_n))]} \quad (1)$$

Where $\omega = 2\pi\nu$ and ν is the microwave frequency, γ is the gyromagnetic ratio, H_R and H_A are the resonance and anisotropy field, ϕ is the angle between the applied field and the magnetization direction, ϕ_n is the angle between the magnetization orientation and the uniaxial anisotropy axis. This uniaxial anisotropy axis is defined parallel to the easy axis, in which case H_A is positive, or perpendicular to the easy plane, in which case H_A is negative. In the limit of a purely magnetostatic origin of this uniaxial anisotropy field the magnitude of H_A is given by $H_A = 2\pi\text{Ms}$ or $H_A = -4\pi\text{Ms}$ for a nanowire

and thin film, respectively. Thus we arrive to the well known conditions:

$$(\omega/\gamma) = H_R + H_A \quad (2a)$$

$$(\omega/\gamma)^2 = H_R(H_R + H_A) \quad (2b)$$

for the conditions of H applied along the uniaxial anisotropy axis (2a) or perpendicular to the axis. Naturally, if the magnetic anisotropy field is positive H_R (given by $\omega/\gamma - H_A$) is smaller than the resonance field in the paramagnetic state: ω/γ . As long as the anisotropy field is small compared with (ω/γ) the angular variation between the condition perpendicular and parallel to the uniaxial anisotropy axis can be approximated by $3/2 H_A$ [27].

If the anisotropy in these polycrystalline samples is assumed to be randomly distributed, then the spectrum should be well described as a superposition of absorptions centered at different resonance fields given by (1) and weighted with a sine of the anisotropy axis angle with a reference coordinate system. In this way the powder spectrum is calculated [15]. Ideally, from the line-shape it is easy to distinguish a randomly distributed easy-axis system of an easy-plane one [27].

In the paramagnetic region, where the anisotropy is negligible, the PM resonance condition is $H_R = \omega/\gamma$. The ESR lineshape depends on whether or not the microwave fully penetrates the sample. The microwave penetration depth, δ , depends on the sample conductivity and magnetic permeability. In poor conductors with grain size smaller than δ the lines can be described as a Lorentzian. In good conductors with $\delta <$ sample size the ESR lineshape turns out to be a mixture of absorption and dispersion (Dysonian).

On the other hand the microwave frequency is not high enough to excite the AFM mode, namely the resonance condition can not be satisfied due to the high exchange field involved. Therefore below T_N , the AFM phase do not show resonance signal [29].

3.1. $\text{La}_{0.67}\text{Ca}_{0.33}\text{MnO}_3$:

In Fig. 1 we show the measured spectra at 34.3 GHz for the $x = 0.33$ sample. At $T = 340\ \text{K}$ the ESR line is characterized by a g-factor of 1.997(3) and shows only a slight asymmetry due to the admixture of absorption and dispersion line-shapes, characteristic of conducting samples. Approaching the FM transition temperature from above ($T_C \approx 271\ \text{K}$) this asymmetry gets more pronounced and leads to a low-field line lobe larger than the high field one, similarly to what was previously reported in $\text{La}_{0.7}\text{Pb}_{0.3}\text{MnO}_3$ [24]. This is an indication that the skin depth is reduced below the average grain size as a result of the higher electric conductivity combined with the larger magnetic permeability observed near the insulating (PM) to metallic (FM) transition. Below T_C the line broadens and deforms significantly, showing a two-peak structure at high fields, clearly noticed in the $T = 267\ \text{K}$, $230\ \text{K}$ and $205\ \text{K}$ spectra.

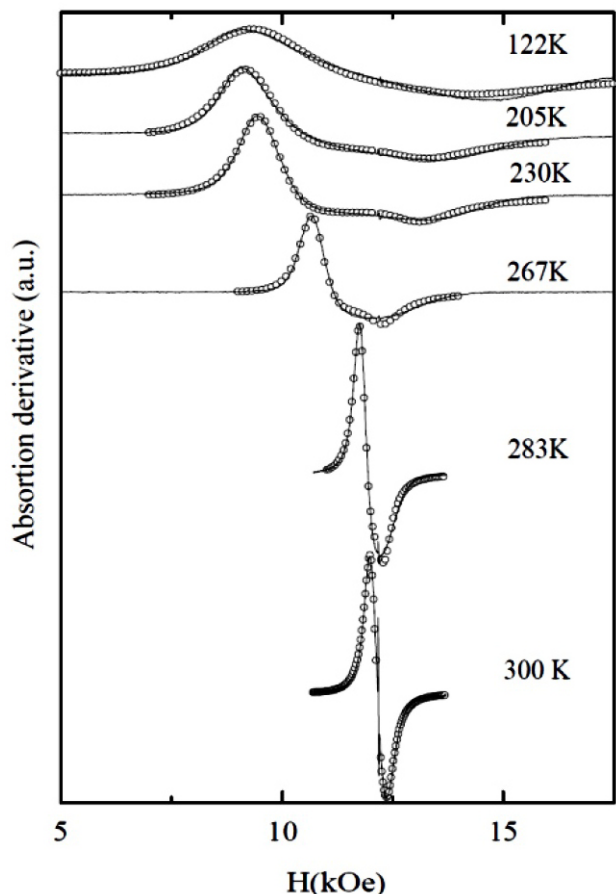


FIGURE 1. ESR spectra of $\text{La}_{1-x}\text{Ca}_x\text{MnO}_3$, $x = 0.33$ at different temperatures. The spectra have been shifted for clarity. The open circles correspond to the fits of the ESR signal to Eq. (1), the full line are the observed spectra.

Also in Fig. 1 we show the fitted spectra using Eq. (1). The fitting function was calculated assuming a randomly distributed uniaxial axis and a mixture of absorption and dispersion lines with weighting factors AP and (1-AP) respectively, and intrinsic width δH . The resulting spectrum is used to adjust H_R , δH , the intensity, AP, and H_A in a non-linear least-square routine [15,27]. The calculated spectrum turns out to have a “two-line” structure. Within this model the low-field maximum is associated with the contributions coming from easy-directions nearly parallel to the applied field, while the high-field structure is due to the contributions near the hard-axis. Thus the peak-to-peak width is related to the anisotropy field. In this way the low-field and high-field structures are linked into a *single* line-structure which is obtained assuming independently additive resonant-line contributions of randomly oriented anisotropy axis.

We note that the line-fits are remarkably good, indicating the plausibility of the model to describe the line-shape.

The results for H_A and AP are given in Fig. 2. The magnitude AP decreases with decreasing T from 0.9 at T = 340 K down to 0.5 at 122 K, the expected value for good conductors in which the skin-depth is smaller than the sample size. As the conductivity and the magnetic permeability both increase

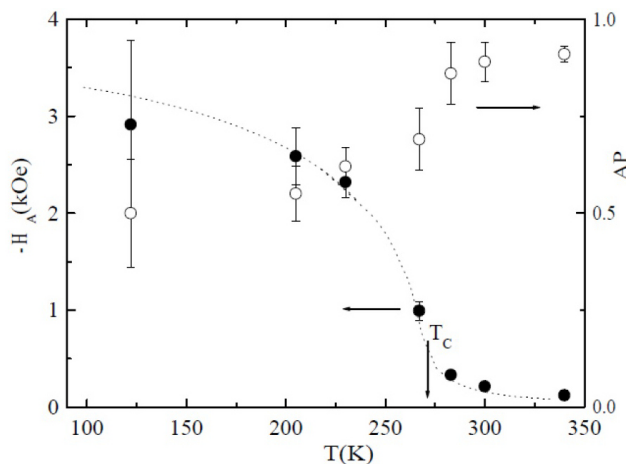


FIGURE 2. $\text{La}_{1-x}\text{Ca}_x\text{MnO}_3$ $x = 0.33$ sample: Anisotropy field determined from the ESR spectra using Eq. (1). The dot-line is the functional dependence of $6Ms(T)$ that describes well the temperature dependence of the anisotropy field. The open circles indicate the absorption proportion (AP) as determined from the ESR line shape (the dispersion proportion is given by $1-AP$).

near two orders of magnitude on going from above T_C to 100 K we expect a large reduction of the skin depth on going from high-T to low-T.

For typical sample grain size, of $L = 10 \mu\text{m}$, $\delta \approx L$ at room temperature. We can expect to observe a crossover to the condition $\delta \ll L$ on decreasing T, as observed.

3.2. $\text{La}_{0.5}\text{Ca}_{0.5}\text{MnO}_3$:

Figure 3 shows the ESR spectra of $\text{La}_{0.5}\text{Ca}_{0.5}\text{MnO}_3$ with $x = 0.5$. As can be observed at room temperature the spectrum is well described by a Lorentzian line centered at $g \sim 2$. For $T < T_C \approx 225$ K a “two-line” structure emerges. These spectra are different from the ones observed for $x = 0.33$ below T_C , in the sense that the low temperature extra structure appears in the low-field side of the spectra. Besides, although magnetization and thermal expansion measurements indicate that a large fraction of an AFM phase is retained upon heating up to $T \approx 193$ K, we did not notice a marked change of the lineshape around this temperature.

In Fig. 3 we also show the calculated spectra using Eq. (1) assuming randomly-oriented anisotropy axis. The fitting parameters were H_A , H_R , and δH . An improvement in the fits were also obtained if the central field was considered to have a narrow Gaussian distribution with $\sigma = 0.05$. This variation of the local effective field could be due to dipolar interactions not taken into account above.

In Fig. 4 we have plotted the anisotropy field obtained from the fits of the ESR lineshape as a function of temperature.

The obtained results can be summarized as follows: i) the full line-shape can be fitted by assuming uniaxial anisotropy field. ii) The sign and magnitude of the anisotropy is different in both samples: for $x = 0.33$ the spectra is consistent with

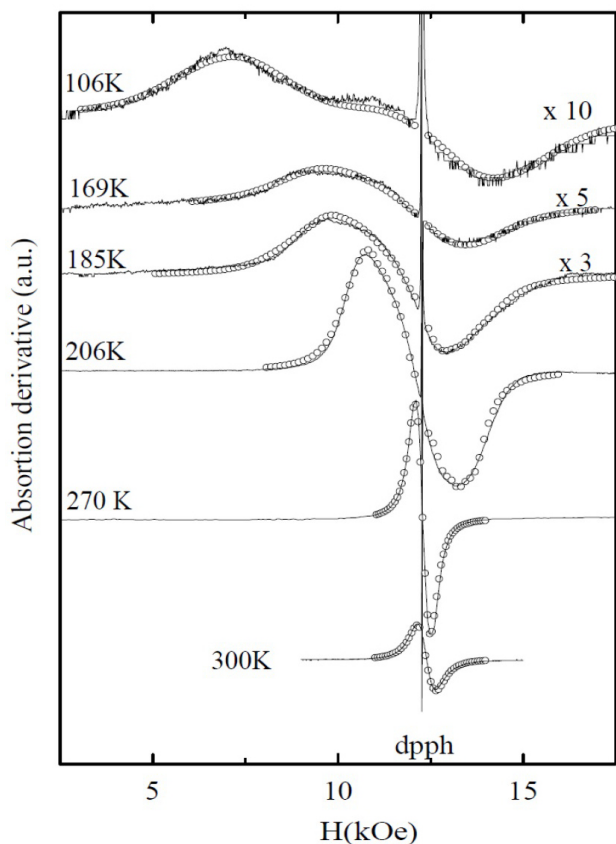


FIGURE 3. ESR spectra of $\text{La}_{1-x}\text{Ca}_x\text{MnO}_3$, $x = 0.5$ at different temperatures. The spectra have been shifted for clarity. The open circles correspond to the fits of the ESR signal to Eq. (1), the full line are the observed spectra.

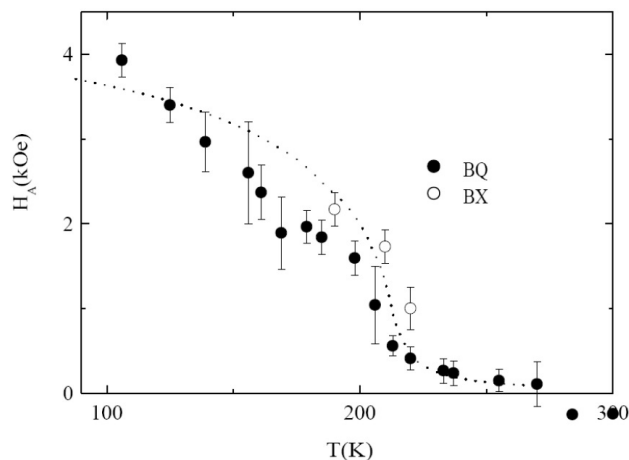


FIGURE 4. $x = 0.5$ sample: Anisotropy field determined from the ESR spectra. The dot line is the estimated shape anisotropy field corresponding to an infinite prolate ellipsoid, $2\pi M_s$.

easy-plane anisotropy; instead for $x = 0.5$, the FMR spectra correspond to easy-axis symmetry. iii) In the $x = 0.33$ sample the lineshape changes from Lorentzian above T_C to Dysonian for T approaching to T_C , in accordance with the increased conductivity and magnetic permeability at low T . These results, represented in Figs. 2 and 4, lead to the following questions: what does it mean that the FMR can be de-

scribed using Eq. (1)? which is the origin of the anisotropy field value?.

The answer to the first question implies that ESR line-shape can be approximated as a collection of spectra each one resonating following their own local anisotropy field, uncoupled (or weakly coupled) from each other. In the case of the $x = 0.5$ sample this result indicates that only a small fraction of the sample is in the FM state, and this fraction decreases with decreasing temperature (yet never totally disappearing). If the fraction of the FM phase is below percolation this would allow each of these FM “islands” to resonate without being significantly exchange-coupled to the other regions. As a result the ESR spectra can be modeled as independent FMR contributions. In the $x = 0.33$ sample, as we mentioned above, the short skin depth limits the region probed by the microwave to the particle surface. For a particle of several μm the coupling between distant regions of the surface must be negligible and therefore they can be approximated as independently resonating regions, even within the same particle.

The answer to the second question requires further discussion. Note, first, that the line-shape depends on the anisotropy sign, which changes from Fig. 1 to Fig. 3. We will discuss first the results of the $x = 0.33$ sample. In this case H_A is negative. If H_A is associated with a shape anisotropy the resonance would correspond to a FM phase with flat ellipsoids shape, which is not likely. However, ESR experiments in metallic magnetic samples probe only a fraction of μm due to the small skin depth. Micromagnetic considerations show that the magnetic moments near a surface tend to align in such a way as to avoid the magnetic moment pointing out of the sample. In terms of a free energy description this effect could be expressed as an easy-plane term of the type $K \cos^2(\phi - \phi_n)$, which is minimum when the equilibrium magnetization lies parallel to the surface, similar to what is found for thin films. This, in turn, leads to an associated negative anisotropy field. Thus stated the effective anisotropy field acting on the alignment of the moments near the surface should be proportional to the magnetization, the coefficient of proportionality depending on the sample shape and surface characteristics. In Fig. 2 we show that the anisotropy field follows the behavior of the magnetization (dotted line).

The above discussion is pertinent for a sample with size larger than the critical size for single magnetic domains. We now turn to the $x = 0.5$ sample. In this sample no sign of dispersion-absorption admixture is found near $T_C = 225$ K indicating that the magnetic regions are smaller than the penetration depth and that the FM domains are small. In this case, if H_A is related to shape anisotropy, it would render information about the shape of the FM domains. The ESR spectra can be described as due to a positive anisotropy field for all temperatures. Interpreting H_A as originated in shape anisotropy we would conclude that the maximum H_A (for a positive value) is $2\pi M_s$: that of an infinite wire.

Considering that M_s follows a similar T -dependence as the one observed for $\text{La}_{0.7}\text{Pb}_{0.3}\text{MnO}_3$ below T_C [24], we calculated the shape anisotropy of a needle-like ellipsoid (dot-

line Fig. 4). Even though this functional form reproduces the tendency of an anisotropy increase with decreasing T, the low-T data points seem to exceed this *maximum* calculated value. Therefore, other mechanisms are required in order to explain the H_A magnitude. Similar results were found recently in other manganites [15,17].

Notice that, while the shape anisotropy field scales as $M(T)$, other uniaxial anisotropy fields (for instance of crystalline origin), are expected to vary as M^2 at low T.

The magnitude of H_A and its large temperature dependence is a confirmation of the need for other sources of anisotropy besides shape.

Several possibilities for the H_A enhancement may be suggested: interface anisotropy, strains, and anisotropies associated with orbital ordering among them. It is well known that interface effects are quite noticeable below 10-20 nm. It is to be expected that as a product of sub-micron phase coexistence, the interface between FM and AFM regions can contribute to the anisotropy value. These interface effects can extend to large regions as the confinement will act at least along the two shortest directions. If indeed the FM/AFM proportion grows with the applied field we would expect the FM regions to become larger with increasing field, and therefore the interface effects should decrease. The small difference observed between the X-band (9.4 GHz) and Q-band anisotropy field may be related to the confinement effect mentioned above. Note also that the large magnetovolume effect observed in this sample [30] indicates that the FM regions have associated a much smaller volume than the AFM regions. This may lead to large strain-induced interface anisotropy in this two-phase system.

Regarding the behavior for $T < T_N$ (Néel temperature ≈ 140 K) we note that the Q-band ESR spectra as a function of T follow a continuous behavior even below T_N : it widens and shifts in a smooth way. This indicates that the ESR signal originates from the same magnetic entity at low T and is not due to the resonance of the AFM phase. The fact that the X-Band signal below T_N is observed to widen and shift to higher fields may be due to the fact that (γH_A) is larger than ω , the exciting microwave frequency. Under this circumstance only a fraction of the sample can be in the saturated resonance condition: only the part that has the anisotropy axis nearly perpendicular to the applied field. The resonance field when the anisotropy axis is exactly perpendicular to the applied field is given by Eq. (2b) which leads to $H_r \approx 4900$ Oe for $(\omega/\gamma) = H_A = 3$ kOe.

This explains the observed shift to higher fields [17,33]. However, we have not attempted to fit the X-Band observed spectra at low T as it is uncertain the way in which the unsaturated part of the sample (the part that has the anisotropy

axis off the perpendicular direction) contributes to the signal.

H_A is a function of the saturation magnetization. Thus, the H_A increase with decreasing temperature suggests that within the FM region the magnetization does not decrease with decreasing T. This is an additional evidence in support of no canting within the FM domain, which corroborates what has been found by neutron scattering [34] and TEM studies using electron holography [7].

4. Conclusions

We have presented Q-Band ESR of $\text{La}_{1-x}\text{Ca}_x\text{MnO}_3$ for $x=0.33$ and $x=0.5$ ceramic samples. The results can be interpreted as due to independently resonating regions subject to an anisotropy field, H_A . The shape of the $x=0.33$ ESR spectra indicates a mixture of absorption and dispersion, with an increase of the latter contribution as the temperature lowers below T_C . The full shape of the spectra can be adjusted assuming a negative anisotropy field. We argue that the negative anisotropy field can be associated with the minimization of the magnetostatic energy at the sample surface, which is the only probe by the microwave. On the other hand the ESR observed in the $x=0.5$ sample can be interpreted as solely coming from FM regions characterized by a strong positive anisotropy field. Our Q-band experiment shows that there is no need to invoke a second resonance (paramagnetic or antiferromagnetic) signal to describe the spectra. Our data is consistent with phase segregation into FM + AFM: as the AFM phase should not contribute to the observed spectra its main effect is the reduction of intensity observed at low temperature. The large value of H_A , while consistent with other published works [15, 17] is intriguing. Shape anisotropy alone cannot account for its low-T behavior, indicating other sources of anisotropy are required to explain the observed values. The large strains originated in the cooperative Jahn-Teller distortions associated to the AFM phase are likely to induce strong crystalline distortions into the FM regions and strain-induced uniaxial anisotropy. We discussed a possible way to interpret ESR spectra in the ordered phase of manganites as due to a uniaxial anisotropy. However, the origin of this anisotropy remains to be explored in future experimental or theoretical work.

Acknowledgements

This work was supported by the ANPCyT PICT-2006 00829, PICTR 20770/04 and UNCuyo C06/320. CAR thanks Prof. J. Rivas and F. Rivadulla for their support and discussions. EW is member of CONICET.

1. M.B. Salamon and M. Jaime, *Rev. Mod. Phys.* **73** (2001) 583.
2. A. Moreo, M. Mayr, A. Feiguin, S. Yunoki, and E. Dagotto, *Phys. Rev. Lett.* **84** (2000) 5568.
3. J. Mira *et al.*, *Phys. Rev. B* **65** (2001) 024418.
4. F. Rivadulla *et al.*, *Phys. Rev. Lett.* **96**(2006) 016402.
5. H. Yoshizawa, H. Kawano, Y. Tomioka, and Y. Tokura, *Phys. Rev. B* **52** (1995) R13145.
6. F. Rivadulla *et al.*, *Phys. Rev. Lett.* **96** (2006) 016402.
7. J.C. Loudon, N.D. Mathur, and P.A. Midgley, *Nature* **420** (2002) 897.
8. E. Wollan and W. Koehler, *Phys. Rev.* **100** (1955) 545.